Robotica (1996) volume 14, pp 561–574. © 1996 Cambridge University Press

Experimental identification of dynamic parameters for a class of geared robots*

Krzysztof R. Kozłowski & Piotr Dutkiewicz

Poznań Technical University, Department of Control, Robotics and Computer Science, ul. Piotrowo 3a, 60-965 Poznań (Poland), email: kk@ar.kari.poz.edu.pl, pdut@ar.kari.poz.edu.pl.

(Received in Final Form: February 22, 1996)

SUMMARY

The main objective of this paper is a presentation of an experimental identification of a non-direct drive robot and load dynamic parameters, which appear in the integral model. The last one is based on the energy theorem formulation. In the robotics literature there are not many experimental results known to the authors, concerning the identification of the dynamic parameters of different models. In order to satisfy this, the experimental system has been built around an industrial ASEA IRp-6 robot. In this paper we propose to precompute the friction characteristics which are separated in the integral model. Various aspects of the exciting trajectories are considered. It is shown how to identify the friction coefficients using a short integral model. The experimental results are presented, including comparison of the results for both integral and differential identification. The identified models are verified by computing the predicted torques and trajectories.

KEYWORDS: Robot dynamics model; Load dynamics model; Friction effects; Parameter identification; Exciting trajectories; Verification of the model.

1. INTRODUCTION

Recently, robot control based on a mathematical model of the nonlinear and coupled arm and gripped load dynamics achieved great importance. As the main purpose of it is the control with high speed and accuracy, the knowledge of the parameters of the dynamics model seems to be very significant. Therefore, many attempts have been carried out in identification of these parameters. Obviously, the simplest way is to take the robot to pieces, and then measure all the details thoroughly.[1] In most cases this is impossible, but when it is, it gives valuable benchmarks for other researchers. More useful are methods, where links of the robot are made to follow the predefined test trajectory.[1-5] The movement parameters (positions, velocities, etc.) are measured simultaneously, and from them the robot and load dynamic parameters can be calculated.

Robot dynamics models can be derived based on the Newton-Euler[1] or Lagrangian formalism.[6] It is well known that both approaches lead to the same dynamical model. Generally, we can consider differential or integral models. The first one is the same as the standard equations of motion for robot dynamics. The friction torques depend on the generalized positions, velocities, direction of the rotation, temperature, and other factors which are very difficult to describe in an analytical form.[7-16] It is assumed that the robot model is canonical,[17-23] which means that the vector, X, of the parameters consists of the minimum number of parameters which are the combinations of the link inertial parameters (namely mass, and first and second moments of the individual links).

Integral models are derived based on the energy theorem, which states that the work of the forces which are applied to the system, and are not derived from a potential, is equal to the change of the total energy of the system.[24-27] Both differential and integral models have the same set of the minimum number of the inertial parameters.[26] In both representations it is assumed that the friction torques, τ_f, are represented by appropriate curves[28,29] and we do not look for the friction coefficients which appear in an approximation of the friction model.

It is usually difficult to measure the friction torques for both differential and integral models. Seeger and Leonhard[12] proposed to measure the friction torques for a class of geared robots, taking the manutec r3 robot as an example. For the same class of robots, but described by an integral model, Kozłowski and Dutkiewicz[8] proposed a method to measure the friction torques. The friction torques depend on the generalized positions, velocities, direction of the rotation, temperature, and other factors.

In the robotics literature there are some experimental studies on off-line robot dynamics estimation.[1,10,24,30-37] Usually industrial robots are equipped with position sensors, seldom with velocity, acceleration and force and torque sensors which are necessary tools to perform identification experiments. In order to obtain velocity and acceleration signals one can differentiate these signals, but this leads to some numerical errors. Not many papers are devoted to the identification of load parameters (namely mass, center of mass and six parameters of the inertia tensor). Some results can be found in Atkeson, An and Hollerbach[1] and Dutkiewicz,

* This paper presents research performed under grant KBN 8 S505 009 06 (from Polish Committee on Scientific Research).

Kozłowski and Wróblewski.[9,38] In order to carry out these experiments the robot has to be equipped with a force and torque sensor.

Some remarks concerning the comparison of the differential and integral models can be found in the work done by Prüfer, Schmidt and Wahl.[26] In this paper we extend these results by considering a design of an optimal trajectory. Generally, one can notice that the differential model is richer in information since all equations for the generalized torques are present. In the case of the integral model (energy model) we deal only with one scalar equation. Because of that the optimal trajectory design for the integral model is more crucial and difficult. It has been noticed that the identification results in case of the integral model appear to be not very sensitive to filtering measurements because of its natural lowpass filter behaviour. Comparing both models from the measurement point of view one can notice that in case of the integral model acceleration signals are not required. In order to avoid acceleration signals in the differential model one can integrate the differential model, but this is not preferred because an integrator is an infinite-gain filter at zero frequency.[10] This means that large errors can result from small low-frequency errors such as offsets. To overcome this shortcoming, a low-pass filter with unit gain at zero frequency can be applied to the differential model.[10,30] In this paper we rather focus our attention on optimal trajectory design for both discussed models.

Different criteria can be used to optimize the input trajectory for the identification experiment. Exciting signals for single-input single-output linear systems were considered by Marrels and coauthors.[39] They proposed to maximize for comparison a minimum singular value, condition number[40] and determinant of the information matrix. The same criteria can be used for the nonlinear systems but one has to be careful with generalization of the results for linear systems. Originally, first operations on finding exciting trajectories for the identification of the dynamic parameters of robot were carried out by Armstrong.[41] He suggested to minimize the condition number or one over the minimum singular value[40] of the information matrix. Vandanjon, Gautier and Desbats[42] proposed the minimization of the Frobenius condition number of the information matrix. A comparison of different criteria of exciting trajectories for robot identification were considered by Presse and Gautier,[43] Gautier and Khalil[44] or Gautier.[45] They proposed a criterion which takes into account *a priori* information about both the measurement vector and knowledge of the solution. Most of the authors propose to minimize the condition number of the information matrix and use it as a criterion of the exciting trajectories for robot identification. Due to lack of *a priori* information mentioned above we have decided to use as a criterion the condition number. We have implemented this criterion for both integral and differential models. Both models are considered for robot parameter identification. For the load identification we have used the differential model with the appropriate optimization scheme. The optimization scheme follows one presented by Armstrong[41] with the extension to the integral model. Some results obtained by the authors were presented by Dutkiewicz and Kozłowski.[46]

The experimental system has been built[47] around an industrial IRp-6 robot, built in Poland under the license of the Swedish ASEA. This is a typical geared industrial robot with five degrees of freedom, driven by DC motors, and with a 16-bit multiprocessor controller. Moreover, the robot is equipped with an external measurement unit enabling monitoring of each axis driving motor's position q_i, velocity $\dot{q}_i$, torque τ_i, as well as with the force/torque sensors, mounted between the wrist of the manipulator and the gripper. During the experiments, the robot was equipped with an American JR3 force/torque sensor.

The main aim of this paper is to show and discuss different aspects of the experimental identification of a class of geared robots (taking the IRp-6 robot as an example) and load dynamic parameters for both differential and integral models. Friction characteristics, which dominate in this class of robots, are widely discussed as well as optimal trajectory design issues. A comparison of two differential and integral models is particularly of interest with applications to robot and load dynamic parameters identification. The paper is organized as follows: In Section II, the differential and integral (for robot and load) dynamic models are presented, including friction effects. In Section III, the identification algorithm will be outlined. In Section IV, different friction characteristics are depicted. In Section V, the experimental results of the differential and integral robot model parameters identification are presented. Friction characteristics, load identification and optimal trajectories are presented too. In Section VI, verification of models is discussed and, finally, concluding remarks end the paper.

2. ROBOT AND LOAD DYNAMICS MODELS

Consider a manipulator structure consisting of n rigid links, numbered in the increasing order from the fixed base (link 0) towards the tip (link n). Joint k connects links $(k-1)$ and k. The system contains only simple revolute and/or prismatic joints; each joint has one degree of freedom. Coordinate frames are assigned according to the modified Denavit–Hartenberg notation.[17]

The dynamic properties of the i-th link of the manipulator are characterized by the inertia tensor ${}^{i}I_i$, the first moment $m_i^i c_i$, and the mass m_i. The friction generalized force acting at the i-th joint is assumed to be of the form (which is a simplified form)

$$\tau_{if}(\dot{q}_i) = F_{iv}\dot{q}_i + F_{ic}\,\mathrm{sign}\,(\dot{q}_i), \tag{1}$$

where F_{iv} is the viscous friction coefficient of the i-th link, F_{ic} is the coefficient of the Coulomb friction (independent of the magnitude of the velocity).

The inertial parameters and the friction coefficients of

the manipulator can be expressed by the $(12n \times 1)$ vector X of robot dynamic parameters

$$X = [I_{1xx}, I_{1xy}, I_{1xz}, I_{1yy}, I_{1yz}, I_{1zz}, m_1, m_1c_{1x}, m_1c_{1y}, m_1c_{1z}, \ldots, I_{nxx}, I_{nxy}, I_{nxz}, I_{nyy}, I_{nyz}, I_{nzz}, m_n, m_nc_{nx}, m_nc_{ny}, m_nc_{nz}, F_{1c}, \ldots, F_{nc}, F_{1v}, \ldots, F_{nv}]^T. \quad (2)$$

where the elements of the inertia tensor and the components of the first moment are self-explanatory and $(\cdot)^T$ denotes the transpose operation. Notice that all parameters are expressed in local coordinate systems and therefore are constant.

Since the total energy of the robot is linear in these parameters,[17,48] formal differentiating of the Lagrangian leads to the following vector equation

$$\tau = D(q, \dot{q}, \ddot{q})X, \quad (3)$$

where $q = [q_1, q_2, \ldots, q_n]^T$ is the vector of generalized coordinates q_i (angular or linear displacements), $\dot{q} = [\dot{q}_1, \dot{q}_2, \ldots, \dot{q}_n]^T$, $\ddot{q} = [\ddot{q}_1, \ddot{q}_2, \ldots, \ddot{q}_n]^T$, $\tau = [\tau_1, \tau_2, \ldots, \tau_n]^T$ is the vector of generalized forces τ_i (force of torque, depending on the type of the joint), and D is a $(n \times 12n)$ matrix, whose elements depend on q, $\dot{q}$, $\ddot{q}$. The so described robot dynamics model is called a differential model. Moreover, we can write

$$E_k = \sum_{i=1}^{12n} \frac{\partial E_k}{\partial X_i} X_i = \sum_{i=1}^{12n} DE_{ki}X_i, \quad (4)$$

$$E_p = \sum_{i=1}^{12n} \frac{\partial E_p}{\partial X_i} X_i = \sum_{i=1}^{12n} DE_{pi}X_i, \quad (5)$$

where X_i is the i-th inertial parameter. DE_{ki} is a function of q, $\dot{q}$, and geometric parameters. DE_{pi} is a function of q and geometric parameters.

Making use of the energy theorem which states that the work of non-potential generalized forces applied to the system is equal to the change of the total energy of the system, it can be written that

$$\int_{t_1}^{t_2} \tau^T \dot{q} dt = (E_k(t_2) + E_p(t_2)) - (E_k(t_1) + E_p(t_1)) = H(t_2) - H(t_1), \quad (6)$$

where $E_k(t_i)$ and $E_p(t_i)$ are the kinetic and potential energy, respectively, of the manipulator at time instance t_i. $H(t_i) = E_k(t_i) + E_p(t_i)$ is the total energy of the system.

Equation (6) can be rewritten in the following scalar form

$$y = \int_{t_1}^{t_2} \tau^T \dot{q} dt = d^T(q, \ddot{q})X, \quad (7)$$

which is linear in the inertial and friction parameters, and vector d depends on q and $\dot{q}$. This does not require a knowledge of joint acceleration, and it is often called the integral model[27] as opposite to the differential model.[3]

Here we make one comment. For the purpose of identification a sufficient number of equations has to be calculated based on equation (7) between different time intervals. One possibility is to calculate the k-*th* equation in the time interval $(t_1, t_2)_k$. Another one is to calculate equation (7) in time interval which starts from $t_0 = 0$ and ends t_f where t_f denotes a final time of calculations. In the first situation we are dealing with a short-time integral, in the second case we have long time integral. We will use widely these definitions in section V describing experimental results.

Now we recall the results for the load dynamic parameters models.[1] The differential model for the load parameters carried by the gripper can be written as follows:

$$W = K\Phi, \quad (8)$$

where $W = [F_x, F_y, F_z, N_x, N_y, N_z]^T$ is a (6×1) vector consisting of force and torque coordinates, expressed in the local coordinate frame of the force/torque sensor. K is a (6×10) matrix of the following form

$$K = \begin{bmatrix} \dot{v} - {}^P_0Rg, & [\dot{\omega}\times] + [\omega\times][\omega\times], & 0 \\ 0, & [({}^P_0Rg - \dot{v})\times], & [\cdot\dot{\omega}] + [\omega\times][\cdot\omega] \end{bmatrix} \quad (9)$$

depending on the load configuration in the base coordinate frame, i.e. on the changes of the vectors $\ddot{p}$, ω, and $\dot{\omega}$. Φ is a (10×1) vector of the load dynamic parameters,

$$\Phi = [m, mc_x, mc_y, mc_z, I_{xx}, I_{xy}, I_{xz}, I_{yy}, I_{yz}, I_{zz}]^T. \quad (10)$$

All the parameters are expressed in the local coordinate frame attached to a load with the origin located at the point P (origin of the local coordinate frame in which forces and torques are measured). $\dot{v}$ is a linear acceleration of the point P, ω and $\dot{\omega}$ are the angular velocity and acceleration vectors of the load, $[\omega\times]$ is a 3×3 skew-symmetric matrix used to perform a cross product operation, $[\cdot\omega]$ is a 3×6 matrix used to calculate a product ωI when six elements of the inertia tensor I are written in a row. Moreover, $g = [0, 0, g_0]^T$ is the gravity vector expressed in the base coordinate frame, and ${}^P_0R$ is the rotation matrix transforming the base coordinate frame to the local coordinate frame with the origin at the point P.

The acceleration signals $\dot{v}$ and $\dot{\omega}$ occurring in equation (9), are difficult to measure. To avoid this, (8) can be integrated in the time interval $(t, t+T)$, where $(t, t+T) = (t_1, t_2)_k$, or $(t, t+T) = (t_0, t_f)$, in the local coordinate frame with the origin at the point P, affixed to the force/torque sensor. In this case the following integral model is obtained.[38]

$$\begin{bmatrix} \int_t^{t+T} F d\tau \\ \int_t^{t+T} N d\tau \end{bmatrix} = \left[\int_t^{t+T} K d\tau\right]\Phi = K_I\Phi, \quad (11)$$

since the vector Φ does not depend on time. Notice that

model given by equation (11) differs from the integral model obtained by making use of the energy theorem mentioned above. The model given by equation (11) was obtained by performing an integration operation on the differential model; nevertheless, we keep a notion of the integral model in this case too. Recall that integration is an infinite-gain filter at zero frequency.[10] The first three rows of the matrix K_I are as follows:

$$K_{I123} = \Big[v\,|_t^{t+T} + \int_t^{t+T} \omega \times v d\tau - \int_t^{t+T} {}_0^P R g d\tau, [(\omega\,|_t^{t+T} \times] + \int_t^{t+T} [\omega \times][\omega \times] d\tau, 0 \Big], \quad (12)$$

and the next three rows are

$$K_{I456} = \Big[0, [(-v\,|_t^{t+T} - \int_t^{t+T} \omega \times v d\tau + \int_t^{t+T} {}_0^P R g d\tau) \times], [\cdot(\omega\,|_t^{t+T}] + \int_t^{t+T} [\omega \times][\cdot \omega] d\tau \Big]. \quad (13)$$

These equations result from the basic relations describing the vectors and their derivatives in different coordinate frames.[38] Notice that linear and angular accelerations do not occur in (12) and (13). The velocities v and ω are expressed in the local coordinate frame. Like the differential model, the integral model is linear in the elements of the vector Φ.

3. IDENTIFICATION SCHEME

The identification scheme for both robot and load dynamic models is the same; it is also the same for integral and differential models. Therefore, only the robot dynamic parameters identification algorithm for the integral robot dynamics (short integral) model will be shortly outlined. Moreover, it will be assumed that the model described by equation (7) is canonical, i.e. it is represented by the minimal set of the inertial parameters, which is the result of the regrouping (categorization) procedure. The least squares method in recursive form[40] will be used as the identification method.

The integral model is given by equation (7) and the goal is to find an estimate for the parameter vector X. In order to identify X, a sufficient number of equations, obtained by calculating the equation (7) in different time intervals, should be used. For the k-th interval $(t_1, t_2)_k$, such an equation has the form

$$y_k = d_k^T X. \quad (14)$$

Recall that y_k in equation (14) is the integral value of the dot product of generalized forces vector τ and generalized velocities vector $\dot{q}$ in time interval $(t_1, t_2)_k$, resulting from the work done by non-potential forces acting on the system. Assuming that k varies from 1 to r and taking into account equation (14), the following equation can be written:

$$y_r = h_r X + w, \quad (15)$$

where w is the observation error vector, $h_r = [d_1, \ldots, d_r]^T$, and $\bar{y}_r = [y_1, \ldots, y_r]^T$. Assuming that $r > M_c$ (M_c is the number of inertial parameters of the canonical model, in general[19] $M_c \neq 7n - 4 + 2n$) the least squares method leads to the formula

$$\hat{X} = (h_r^T h_r)^{-1} h_r^T y_r. \quad (16)$$

The condition for the solution of this equation to exist is that matrix h_r be positive definite. The recursive solution of equation (16) has the following form:[2]

$$\hat{X}_{L+1} = \hat{X}_L + P_{L+1} d_L (y_L - d_L^T \hat{X}_L), \quad (17)$$

$$P_{L+1} = P_L - (1 + d_L^T P_L d_L)^{-1} P_L d_L d_L^T T_L, \quad (18)$$

where $P_L = (h_L^T h_L)^{-1}$. With the solution known for L equations, the next step solution can be obtained using y_L and d_L, calculated in the time interval $(t_1, t_2)_L$. A common choice of the initial values in these equations is $P_0 = cI$ and $X_0 = 0$, where c is a constant and I is the identity matrix. As mentioned before for the k-th equation (7) different lengths of the time interval $(t_1, t_2)_k$ may be assumed. In the case when $t_1 = t_0$ and $t_2 = t_k$, the observation of equation (7) is performed from the start with a growing time interval.

4. FRICTION CHARACTERISTICS

In Section 2 we have introduced a very simple friction model given by equation (1). Here we show more insights into friction modelling. It has been established, that friction depends on the direction of rotation, as well as on the temperature. Armstrong[7] studied different friction models. Most of them are based on the Tustin model. Usually researchers assume the existence of dry and velocity dependent parts in the friction phenomena.[1,10,12,49] Very seldom authors analyze the friction coefficients as a function of temperature changes.[7,16,26] which is particularly important for geared robots. These robots are equipped with different mechanical gears such as harmonic drives, which change their characteristics with temperature.

Friction models have been extensively studied in the literature. These models established, that the torque is a function of the angular velocity. The most accurate is the Tustin's model (exponential model).[7] In this section we propose a simple experimental method, which allows one to model the exponential friction characterization at a wide range of velocities for a geared robot. Assume now that to the right hand side of equation (3) friction torques, τ_f, are added (compare equation (21)). If we multiply both sides of this new equation by $\dot{q}$ and next integrate from t_1 to t_2 we get the following equation:

$$\int_{t_1}^{t_2} \tau^T \dot{q} dt = H(t_2) - H(t_1) + \int_{t_1}^{t_2} \tau_f^T \dot{q} dt. \quad (19)$$

Notice that multiplication of $X^T D^T(q, \dot{q}, \ddot{q})$ by $\dot{q}$ results in $H(t_2) - H(t_1)$ (the integral model can be obtained equivalently as just described). Notice that the vector τ_f incorporates Coulomb and viscous friction coefficients (compare equations (1)) and all the other friction phenomena.

In order to measure the friction torque we propose the following method:

- The i-th link is moved alone with constant velocity (possible the smallest). During the movement, the corresponding current is measured, as well as the desired constant velocity and position.
- The velocity is incremented by $\Delta\dot{q}$ and the procedure described in the first point is repeated.
- The procedure is terminated when the maximum velocity for the i-th link has been achieved.

The assumption of the constant velocity leads to the situation in which the difference between the kinetic energy in equation (19) vanishes. For the column of the robot there is no gravitation, and the difference of the potential energy vanishes. For other joints in order to make the difference of the potential energy equal to zero one can move a joint with constant velocity in a small vicinity around a given position (we recognize the direction of the movement, which is consistent with the assumption that the friction depends on the direction of the rotation). Making use of the above assumptions we can rearrange equation (19) as follows

$$\tau_f|_{q=const} = \frac{\int_{t_1}^{t_2} \tau_i dt}{t_2 - t_1}. \tag{20}$$

If it is not possible to keep the constant velocity during the movement, one can average the measured velocity signal during its movement. A similar approach has been implemented for the differential model of the Manutec robot by Seeger and Leonhard.[12] In this situation equation (3) has the following form

$$\tau = D(q, \dot{q}, \ddot{q})X + \tau_f \tag{21}$$

where vector X does not contain the friction coefficients. Having precomputed friction characteristics one can subtract the term $\int_{t_1}^{t_2} \tau_f^T \dot{q} dt$ from the right-hand side of equation (19) (or term τ_f in equation (21)) and perform an identification procedure.

5. EXPERIMENTAL RESULTS

The main part of an experimental set-up consists of the IRp-6 robot. This is a typical industrial robot with five degrees of freedom, driven by DC motors. The IRp-6 robot (which represents a class of geared robots) has a gear mechanism in which harmonic drives are used. There are three of them, which move the base of the robot, arm and foream. In order to improve lubrication of the gear mechanism, the harmonic drive, which moves the base of the robot, is embedded in oil, and two others are lubricated by grease. These details are important and different experimental schemes have been applied to these harmonic drives.

The industrial robot controller is based on a 16-bit microprocessor, while each of the motors is controlled by a 8-bit microprocessor card. In order to have a fast and direct access to the robot controller hardware, a parallel 16-bit interface between a PC/AT-486 host computer and the robot controller has been used. Each motor's position, velocity, and current can be measured by means of a resolver, a tachometer, and an external measurement unit, enabling monitoring (with a sampling rate of 0.5 ms) of axis positions q_i, velocities $\dot{q}_i$, and currents of the DC motors of the robot, which are proportional to the driving torques τ_i.

A strain gauge force/torque sensor is used to measure, in the local coordinate frame, coordinates of force and torque exerted at the load gripped by the robot. The sensor is mounted between the wrist of the manipulator and the gripper. During the experiments, the robot was equipped with American JR3 force/torque sensor. The sampling frequency of the JR3 sensor is 250 Hz. The JR3 sensor is especially appropriate for industrial applications due to its inaccuracy and noise resistance.

5.1 Robot parameters identification

The experimental identification of the IRp-6 robot inertial and friction parameters has been carried out for the first three links. A complete kinematical structure of the IRp-6 robot according to the modified Denavit–Hartenberg notation is presented in Fig. 1. The prerequisites of successful identification are the canonical model and trajectories fulfilling the persistent exciting condition. The parameterization of the IRp-6 robot dynamics integral model leads to 13 aggregated

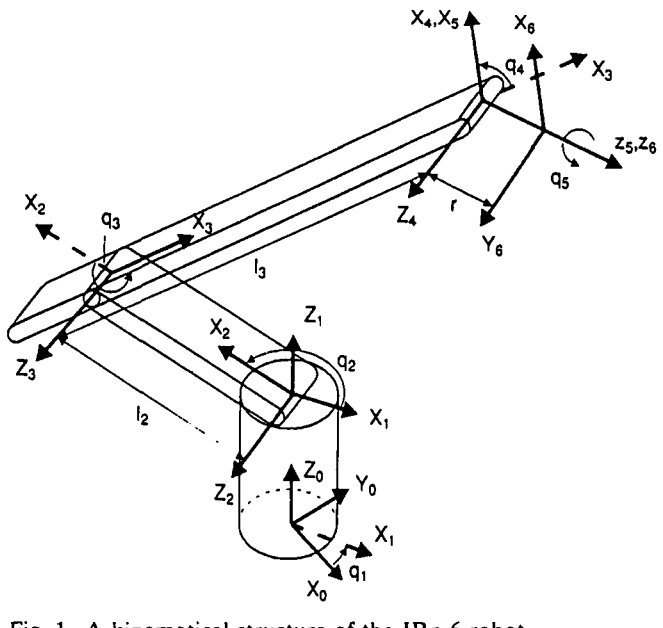

Fig. 1. A kinematical structure of the IRp-6 robot.

parameters $X_1, \ldots, X_{13}$ and accompanying expressions d_i (see: equation (7)). They are as follows:

$$X_1 = I_{1zz} + I_{a1}n_1^2 + I_{2xx} + I_{3yy}$$

$$X_2 = I_{2yy} - I_{2xx} + m_3 l_2^2 - I_{3yy} + I_{3xx}$$

$$X_3 = I_{2zz} + \left(\frac{dF_2}{d\phi_2}\right)^2 I_{a2} + I_{3zz} + \left(\frac{dF_2}{d\phi_3}\right)^2 I_{a3} + l_2^2 m_3$$

$$X_4 = I_{3zz} + \left(\frac{dF_3}{d\phi_3}\right)^2 I_{a3}$$

$$X_5 = I_{3yy} - I_{3xx}$$

$$X_6 = m_3 c_{3x}$$

$$X_7 = m_2 c_{2x} + l_2 m_3$$

$$X_8 = F_{1c}$$

$$X_9 = F_{2c}$$

$$X_{10} = F_{3c}$$

$$X_{11} = F_{1v}$$

$$X_{12} = F_{2v}$$

$$X_{13} = F_{3v}$$

$$d_1 = \frac{1}{2}\dot{q}_1^2$$

$$d_2 = \frac{1}{2}\dot{q}_1^2 \sin^2 q_2$$

$$d_3 = \frac{1}{2}\dot{q}_2^2$$

$$d_4 = \frac{1}{2}\dot{q}_3^2 + \dot{q}_3^2 + \dot{q}_2\dot{q}_3$$

$$d_5 = -\frac{1}{2}[\sin^2(q_3)\cos(2q_2) + \frac{1}{2}\sin(2q_2)\sin(2q_3))\dot{q}_1^2$$

$$d_6 = l_2 \sin q_3(\dot{q}_2 + \dot{q}_3)\dot{q}_2 - l_2 \sin q_2 \cos(q_2 + q_3)\dot{q}_1^2 + g \sin(q_2 + q_3)$$

$$d_7 = g \cos q_2$$

$$d_8 = \int |\dot{q}_1| dt$$

$$d_9 = \int |\dot{q}_2| dt$$

$$d_{10} = \int |\dot{q}_2 + \dot{q}_3| dt$$

$$d_{11} = \int \dot{q}_1^2 \, dt$$

$$d_{12} = \int \dot{q}_2^2 \, dt$$

$$d_{13} = \int (\dot{q}_2 + \dot{q}_3)^2 dt$$

where I_{ai} is the actuator inertia moment of the i-th link, and l_2 is a geometric constant of the 2-nd link. n_1 is the gear ratio of the first actuator, and $dF_2/d\phi_2$, $dF_3/d\phi_3$ are nonlinear functions describing the gear ratios of the 2-nd and 3-rd link actuator, respectively. These functions have the following form

$$\frac{dF_2}{d\phi_2} = \frac{\pi}{SK} \frac{x_1^2 \cos(\beta - \phi_{20} - \phi_2)}{\sqrt{x_2^2 - x_1^2 \sin(\beta - \phi_{20} - \phi_2)}},$$

$$\frac{dF_3}{d\phi_3} = \frac{\pi}{SK} \frac{x_1^2 \cos(\beta - \phi_{30} - \phi_3)}{\sqrt{x_2^2 - x_1^2 \sin(\beta - \phi_{30} - \phi_3)}},$$

in which $\phi_2 = -q_2$ and $\phi_3 = q_2 + q_3$ and x_1, x_2, β, ϕ_{20}, ϕ_{30}, and SK are constants associated with complicated drive mechanism. Details can be found in reference 31. We have assumed that these functions are constant during identification experiments (in reality they change within the range $165 \div 170$ in the whole range of q_2 and q_3 coordinates). An identification of all 13 parameters during simultaneous movement of the three links, using both short and long integral, was not completed successfully. Only 10 parameters were properly identified; for other parameters the d expressions appeared to be strongly linearly dependent.

The identification with the differential model was also not successful. The explanation of this fact is as follows: Friction coefficients, namely parameters $X_8 \div X_{13}$ are dominant in the model. They are responsible for the linear relationship between the functions associated with them. This was also observed by Szynkiewicz, Gosiewski and Janecki in their work.[31] Furthermore, we were not able to move the IRp-6 robot fast enough in order to excite all parameters. This hypothesis was verified later on by numerical results of the optimization procedure (compare section V.4),

Because of this only movements of single joints as well as simultaneous movements of two joints were executed. During the movement of the 1-st joint 3 aggregated parameters can be obtained (namely X_1, X_8, and X_{11}), during the movement of the 2-nd joint 4 parameters (namely X_7, X_8, X_{12}, and part of X_3: $I_{2zz} + (dF_2/d\phi_2)^2 I_{2a} + m_3 l_2^2$), and during the movement of the 3-rd joint also 4 parameters can be obtained (namely X_4, X_6, X_{11}, and X_{13}). The simultaneous movement of the 1-st and 3-rd joints allows identifying of 8 aggregated parameters (namely X_1, X_5, X_6, X_8, X_{10}, X_{11}, X_{13} and part of X_3: $I_{3zz} + (dF_3/d\phi_3)^2 I_{a3}$). Notice that the performing movements described above one can identify all dynamic parameters of the IRp-6 robot. A parameter x_{27} was not identified because it was very small and can be neglected. This is reasonable assumption (cf. Seeger and Leonhard).[12] Parameter X_3 is completely identified during second and fourth movements as a sum of partial results of the identification. Notice that all parameters except X_3 can be identified separately and we avoid an accumulation of errors which might appear in a sequential identification.[23,24,29,33] In our case this is due to the kinematical structure of the IRp-6 robot. The identification procedure proposed in this paper with friction characteristics measurements described in the

next subsection gave better results than those obtained by Szynkiewicz, Gosiewski, and Janecki.[31] As an example, take the data measured during the movement of the 2-nd link which allow one to obtain the following aggregated parameters X_i and the d_i expressions (here, just for simplicity, we number the parameters and associated with them d functions starting from 1 which does not necessary reflects the numbers for a complete model described above):

$$X_1 = m_2 c_{2x} + m_3 l_2$$

$$X_2 = I_{2zz} + \left(\frac{dF_2}{d\phi_2}\right)^2 I_{a2} + m_3 l_2^2$$

$$X_3 = F_{2v}$$

$$X_4 = F_{2c}$$

$$d_1 = g_0 \cos q_2$$

$$d_2 = \frac{1}{2}\dot{q}_2^2$$

$$d_3 = \int \dot{q}_2^2 \, dt$$

$$d_4 = \int |\dot{q}_2| \, dt$$

As an example, identification results for the 2-nd link will be presented. The test trajectory consists of splined polynomials of the 5-th order. The estimates $\hat{X}_1$, $\hat{X}_2$, $\hat{X}_3$, and $\hat{X}_4$ of the aggregated parameters are equal to $\hat{X}_1 = 8.125$ kgm, $\hat{X}_2 = 5.5$ kgm^2, and the friction parameters $\hat{X}_3 = 26$ Nms, and $\hat{X}_4 = 28.75$ km. The estimates, calculated using (17), settle in the time of $1 \div 1.5$ s, and 8000 samples have been measured for one movement.

The presented results were calculated using a short integral (with the step of 5 ms). The results of a long integral were significantly worse, as in this case the errors of the measurements of $\dot{q}$ and τ were accumulated. The results of the differential model were of a similar nature.

5.2 Friction characteristics measurements

A general procedure to measure the friction characteristics has been described in the previous section. Nevertheless, a different scenario has been proposed for the link at the base of the manipulator. It has been observed, that due to the presence of oil in the harmonic drive, the friction characteristic depends on the temperature. The temperature has been changed from 20°C to 45°C. For the arm and forearm of the IRp-6 robot this phenomenon has not been observed.

As it was already pointed out for the base of the manipulator there is no gravitation. This situation changes for the second and third link. We have placed the second link in vertical position and calibrated it with high accuracy. Then the second link was moved with constant velocity from its vertical position in both directions. In order to neglect the potential energy, which is present on the right hand side of equation (19), the movement was designed to be symmetric with respect to the vertical position of the link (and robot at the same time) from its left hand side position, with respect to the vertical position, to its right hand side, and *vice versa*. Going back and forward was necessary in order to recognize the direction of the rotation of the link itself.

A slightly different scenario was proposed for the third link. The link itself was placed in its horizontal position and balanced. The link is balanced by the manufacturer but in our experiment, in addition, counter-balance was carefully tuned. Next, the movement around its horizontal position was introduced in similar fashion as for the second link. The direction of rotation was recognized. For each link movement in one direction 11 points were recorded. The velocity was changed from 5% of the maximum velocity up to 100% of the maximum velocity through 10% with a step 10%. For each movement position, velocity, and current were measured with 1 msec, as a discrete time step. The integral in equation (20) was calculated every 0.5 sec. for the first and the 0.3 sec. for the second and third joint. Values 0.3 sec. and 0.5 sec. were depicted experimentally in such a way that they guarantee a constant temperature during the experiment. This means that on average, for each velocity point, 500 points of the currents were recorded in order to calculate the integral in equation (20). Regardless of the measurement system constant velocity was checked by calculating the increment of the path in degrees divided by an increment of time. This procedure ensures a constant velocity for each point. The time 0.5 sec. was obtained experimentally in order to keep a constant temperature during the experiment.

For each joint the sticktion friction in both directions has been measured. In order to observe this phenomenon for each increment, motor positions were inputted to the controller, and at the same time a torque was measured by the force/torque sensor in contact with rigid environment. When tested joint started to move the measured torque was recorded as a sticktion friction.

For the first joint in both directions the sticktion torque is 14.1 Nm. For the second joint the sticktion torque in positive velocity direction is 16.8 Nm and in

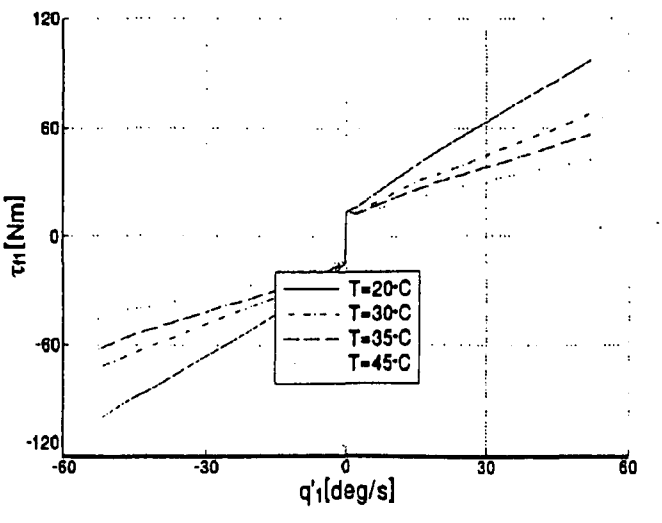

Fig. 2. Friction torques versus velocity for the first joint.

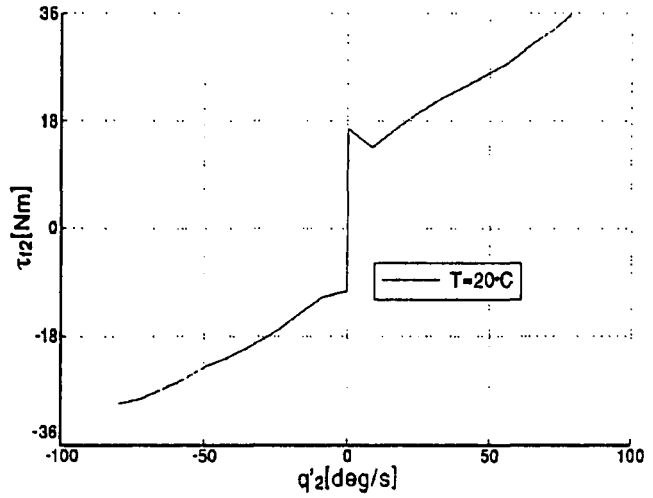

Fig. 3. Friction torque versus velocity for the second joint.

negative direction is 10.6 Nm. For the third joint these numbers are 18.0 Nm and 14.1 Nm, respectively.

In Fig. 2 the friction torques versus velocity for the first joint are presented. One may notice, that the friction torque depends on the temperature. In Figs. 3 and 4 the friction torques for the second and third joint are presented. During the experiment it was observed, that at low velocities the friction torque first decreases and later increases, as described in Tustin's model.

The friction characteristics presented in Figs. 2–4 were used in the identification scheme of the mass parameters of the IRp-6 robot. In the identification process we have moved each joint of the robot separately in order to minimize the number of parameters to be identified. As mentioned above, the friction characteristics were used as precomputed curves and plugged into equation (19). Next the mass parameters were identified. We repeated this procedure for all joints. Here we present only the results for the first joint. The identified mass parameter for the first joint is presented in Fig. 5.

Notice that the estimate is stable in comparison with the situation when additionally two friction coefficients

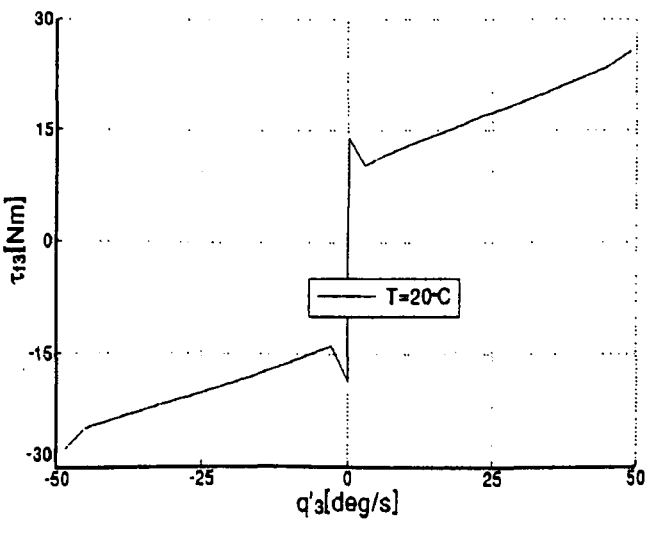

Fig. 4. Friction torque versus velocity for the third joint.

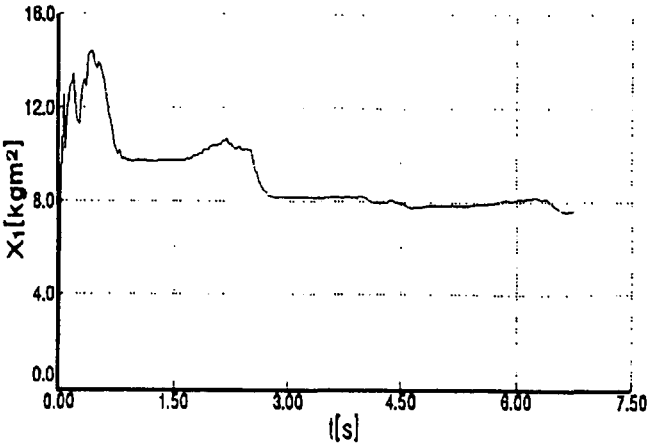

Fig. 5. Mass parameter estimate of the first link.

are included in the identification process. The results for the other joints are of a similar nature.

5.3 Load parameters identification

All the parameters were estimated using the JR3 sensor. Firstly, the differential model with dynamic parameters, described by equation (8), has been used.[28] As an example, the identification results of a steel cuboidal load are presented. Its dynamic parameters are easy to calculate using its measured mass and geometric parameters. Dynamic parameters, presented in Table I, were determined in the local coordinate frame, assigned to the force/torque sensor.

Since the velocity signals, measured using tachometers, are not sufficiently accurate, the position signals were numerically differentiated and compared to the velocity signals. They appeared to be more accurate, even for a simple 3-point differentiating filter, with a sample interval of $\Delta t = 32ms$. The acceleration signal was obtained by differentiating the velocity. It was assumed that the movement of each joint was described by a polynomial of the 5-th order in the joint coordinates. The ranges of the movement were as follows: $-40° \leq q_1 \leq 30°$, $10° \geq q_2 \geq -20°$, $-30° \leq q_3 \leq 40°$, $30° \geq q_4 \geq -10°$, $-150° \leq q_5 \leq -10°$.

The time of the movement was equal 1.83 s for each joint. Comparing the estimates to the computed values (see Table I), it can be noticed that the mass and the static moment were estimated exactly. The estimates of the inertia products, smaller than the inertia moments, are worse, though the results do not differ significantly from the computed values. By repeating the measurement 30 times, the standard deviation was obtained. The results show that the data has a good reliability from the statistical point of view (small standard deviation). This means that should the model be correct the true values of the dynamic parameters can be precisely identified with high confidence level (in our case of 99%).[10]

The movement of the robot arm during the identification measurements was the fastest possible. During slow movements, it was only possible to identify mass and static moment. It is obvious that it was impossible to identify the inertia tensor elements in such

Table I Dynamic Parameters of the Load

Parameter	Computed Values	Estimated Values	Standard Deviation	Confidence Interval
m [kg]	1.910	1.916	0.024	0.011
mc_x [kgm]	0.0573	0.0568	0.0028	0.0013
mc_y [kgm]	−0.0210	−0.0207	0.0088	0.0042
mc_z [kgm]	0.1394	0.1396	0.0091	0.0044
I_{xx} [kgm^2]	0.01050	0.01186	0.0051	0.0024
I_{xy} [kgm^2]	0.00094	−0.00083	0.0014	0.00067
I_{xz} [kgm^2]	−0.00450	−0.00751	0.0017	0.00084
I_{yy} [kgm^2]	0.01635	0.01567	0.0071	0.0034
I_{yz} [kgm^2]	0.00169	0.00001	0.00060	0.00029
I_{zz} [kgm^2]	0.00520	0.00449	0.00037	0.00018

case. As the trajectories polynomials of the 3-rd and 5-th order have been used, both with good results. Some problems have been met when using the integral model, described by equation (11). Generally, when both "short integrals" and "long integrals" were used, the parameter estimates were worse than for differential model, and the set of scalar equations had tendencies to linear dependencies. As a consequence of integration, large errors coming from cumulated low-frequency measurement disturbances have been obtained. When only some of scalar equations from vector equation (11) have been used, the results were significantly better.

5.4 Exciting trajectories

To improve the accuracy of the identified parameters we have run a program which calculates optimal trajectories (for the test movements described in subsection V.1) according to the scheme presented by Armstrong[41] and then we extended these results to the integral model.[46] First, we have implemented differential model calculations for all joints of the IRp-6 robot. The initial value of the condition number for a test trajectory was 10^{14}. After 90 iterations the condition number was 10^{13}. The optimization procedure for these iterations took about 20 hours of CPU time of an IBM 486 compatible computer. Generally speaking, for all three joints of the IRp-6 robot we have not obtained good results out of the optimization procedure. Next we have considered equation (21) for $i = 1$. We assumed that starting trajectories for the first and second joints were spline polynomials and for the third joint was a cosine function. The initial value of the condition number was $1.9 \cdot 10^5$, and after 88 iterations its value was about 88. The optimal trajectory was calculated at 300 points. As an example the results of the optimization procedure are shown in Figure 5. Here we do not plot condition number over time because its behaviour is similar to that presented for differential model by Prüfer, Schmidt, and Wahl.[26] Notice also from Figure 6 that the acceleration for the second joint is not realizable due to IRp-6 acceleration constrains. The same situation was observed for other links. Because of that it was not possible to carry out experiments with optimal trajectories for differential model. Next we have run numerical calculations for the integral model. In that case we have made use of a *Mathematica* package[50] and run all programs on an IBM compatible computer. The results for all three joints were not satisfactory. Therefore we have run several experiments moving only one joint and keeping other joints idle.

For numerical experiments we have used equation (19). Moving the second joint only and not actuating the first and second joints, and assuming a cosine input trajectory for the second joint, we have obtained the initial value of the condition number about 3000. After

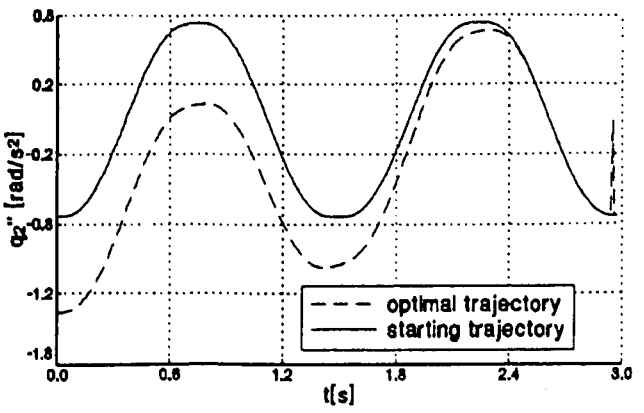

Fig. 6. Starting and optimal trajectories for the second joint: differential model.

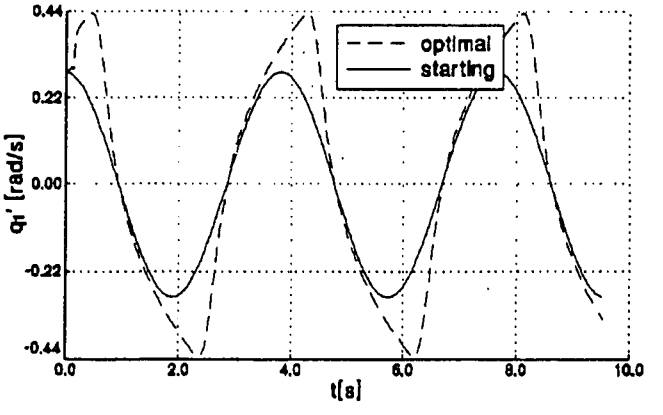

Fig. 7. Starting and optimal trajectories for the first joint: integral model.

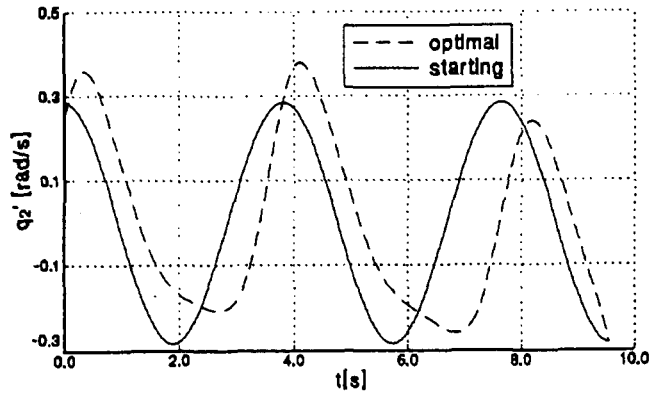

Fig. 8. Starting and optimal trajectories for the second joint; integral model.

about 23 iterations this value changed to 500. The starting and optimal trajectories in this case are shown in Figures 7, 8 and 9.

Notice that in the case of integral model we did not neglect the friction coefficients in equation (19). Most of the authors (for example see Prüfer, Schmidt, and Wahl,[26]) indicate the difficulties in the estimation of the friction coefficients both in the identification scheme and in the optimization procedure. The friction coefficients cause a linear dependence of the parameters. The aim of this paper was to overcome these difficulties.

Finally, we have run numerical calculations for optimal trajectories for load identification. Here we have developed a software package written in *C* language by making use of an object programming technique. In that case we have run several numerical experiments by making use of differential initial trajectories. We have tried spline polynomial trajectories, cosine and many others. It was more difficult to find a good trajectory due to the fact that for load identification we have to choose five joint positions q_i. The problem is bigger in size and takes more computation time. Generally speaking, it is more difficult to identity the load parameters due to fact that joint position, velocities and accelerations are very much limited in size for the IRp-6 robot. The best results were obtained by using the following joint positions (from which joint accelerations, required as input trajectories for the optimization procedure, can be easily calculated):

$$q_1 = 12 - 0.7\cos(0.4\pi + 1.7\alpha) + 0.8\sin(0.1\pi + 0.8\alpha)$$

$$q_2 = 4 + 1.8\cos(0.4\pi + 1.7\alpha) + 1.3\cos(0.1\pi + 0.3\alpha)$$

$$q_3 = 8 + \cos(0.45\pi + 1.4\alpha) + 0.4\sin(0.4\pi + 0.4\alpha) + 0.7\sin(0.8\pi + 0.6\alpha)$$

$$q_4 = 13 - 1.2\sin(0.45\pi + 1.7\alpha) + 1.8\cos(0.15\pi + 0.7\alpha)$$

$$q_5 = -9 + 2.6\cos(0.15\pi + 2\alpha) + 1.1\sin(0.45\pi + 0.2\alpha)$$

where $\alpha = 2\pi(i/K - 1)$, $K = 200$, $i = 0.1 \cdots K - 1$. The initial value for this set of trajectories was 90830 and after 40 iterations went down to about 3000. Starting from this point it was not possible to improve the condition number. For each trajectory we have calculated 200 points with sampling instant $\Delta t = 32ms$. The optimization procedure took about 60 hours of computation time of the IBM-486 compatible computer. The numerical results are shown in Figures 10 to 14.

The exciting trajectories were implemented for the identification of robot inertial parameters as is shown in the next section.

6. VERIFICATION OF THE MODEL

In this section we present experimental results of the identification of the inertial parameters of the IRp-6 robot. As mentioned before, these results were reported by Dutkiewicz, Kozłowski and Wróblewski[9] where the trajectories were chosen in an intuitive way. In this paper we have tried both differential and integral models. Here we present only the results for one joint of the integral model. The short integral model (with $\Delta t = 5$ msec.) is of interest particularly because of its friction coefficients. Some authors (Prüfer, Schmidt and Wahl[26]) claim that it is difficult to identify the friction coefficients due to the fact that they easily become linearly dependent in the identification process. We have observed that this does not have to be true. Using equation (7) and moving only

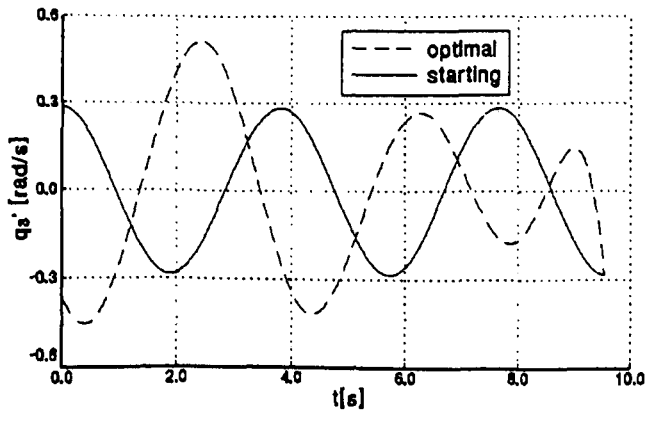

Fig. 9. Starting and optimal trajectories for the third joint; integral model.

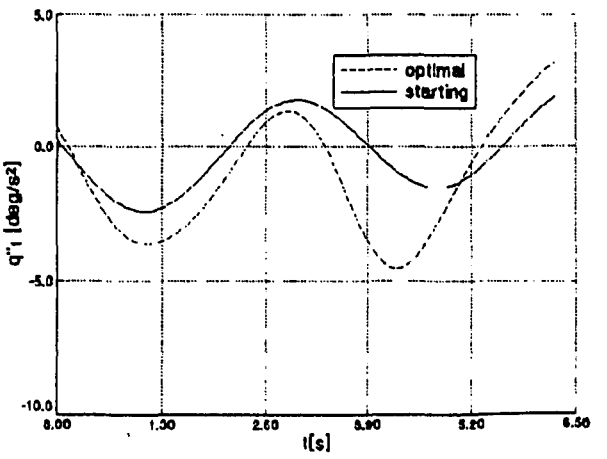

Fig. 10. Starting and optimal trajectories for the first joint; load identification.

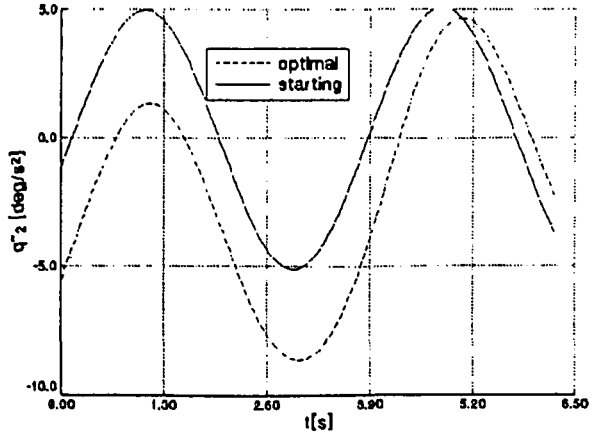

Fig. 11. Starting and optimal trajectories for the second joint; load identification.

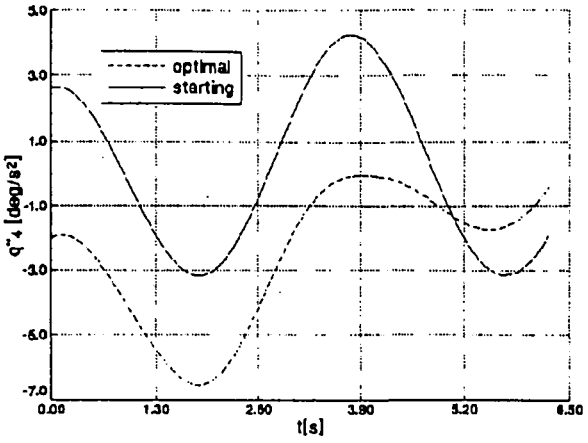

Fig. 13. Starting and optimal trajectories for the fourth joint; load identification.

the first joint we get the following aggregated parameters and the corresponding d functions

$$X_1 = I_{1zz} + I_{a1}n_1^2 + I_{2xx} + I_{3yy} \quad d_1 = \frac{1}{2}\dot{q}_1^2$$

$$X_2 = F_{1c} \quad d_2 = \int |\dot{q}_1| dt$$

$$X_3 = F_{1v} \quad d_3 = \int \dot{q}_1^2 dt$$

where F_{1c} and F_{1v} denote the Coulomb and velocity dependent friction coefficients and other quantities are self-explanatory. Here we have not precomputed the friction torque, because we wanted to check the quality of identification with exciting trajectories. Fortunately, by moving different IRp-6 joints we were able to identity all mass and friction parameters and none of them was involved in two separate movements. This allows one to aovid the accumulated errors during the identification sequential process (compare work done by Presse and Gautier,[23] and Canudas de Wit and Aubin).[51] The identification results are shown in Figures 15a, 15b, and 15c.

From the curves presented in Figures 15a, 15b, and 15c one may note that the estimates are stable when making use of the exciting trajectories. The values of the friction coefficients are very close to the precomputed friction coefficients obtained by Kozłowski and Dutkiewicz.[8,46] This validates the exciting trajectories for the purpose of the identification of the inertial parameters. The results for the other joints were of a similar nature.

The accuracy of the estimation is also verified by comparing the measured joint torques with the predicted torques using the identified parameters. As shown in Figure 16, for the third joint, the predicted torques match the measured (actual) torques closely. This means that our model accurately reflects the dynamic relationship of the robot.

We have also compared the measured–real and simulated–modelled (calculated by solving a set of differential equations describing the robot model with estimated dynamic parameters) joint positions. These positions for the first joint are presented in Figure 17.

The results in that case show good agreement of the simulation with the measured behaviour. In both cases the results for other joints are of a similar nature. Here we make one comment. Authors seldom compare the

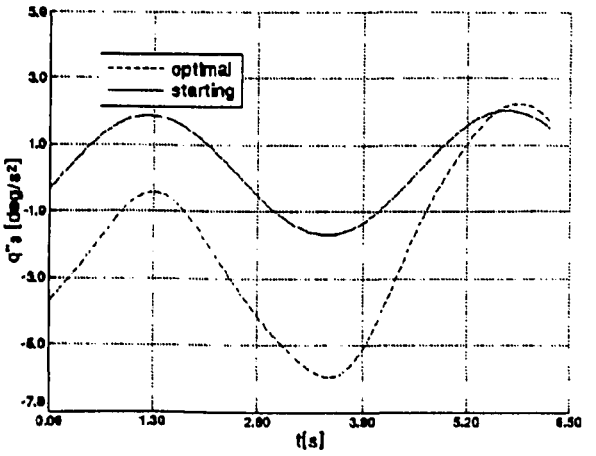

Fig. 12. Starting and optimal trajectories for the third joint; load identification.

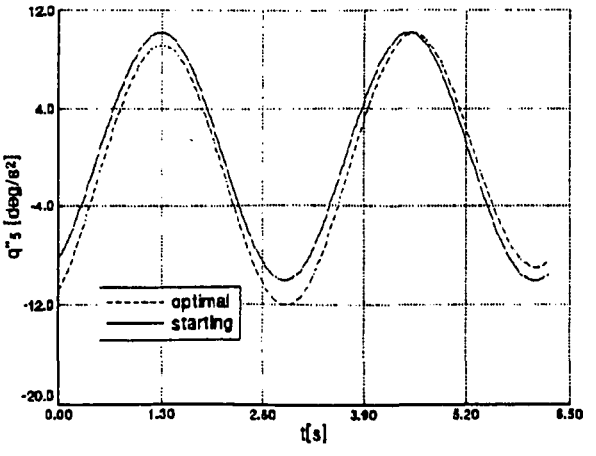

Fig. 14. Starting and optimal trajectories for the fifth joint; load identification.

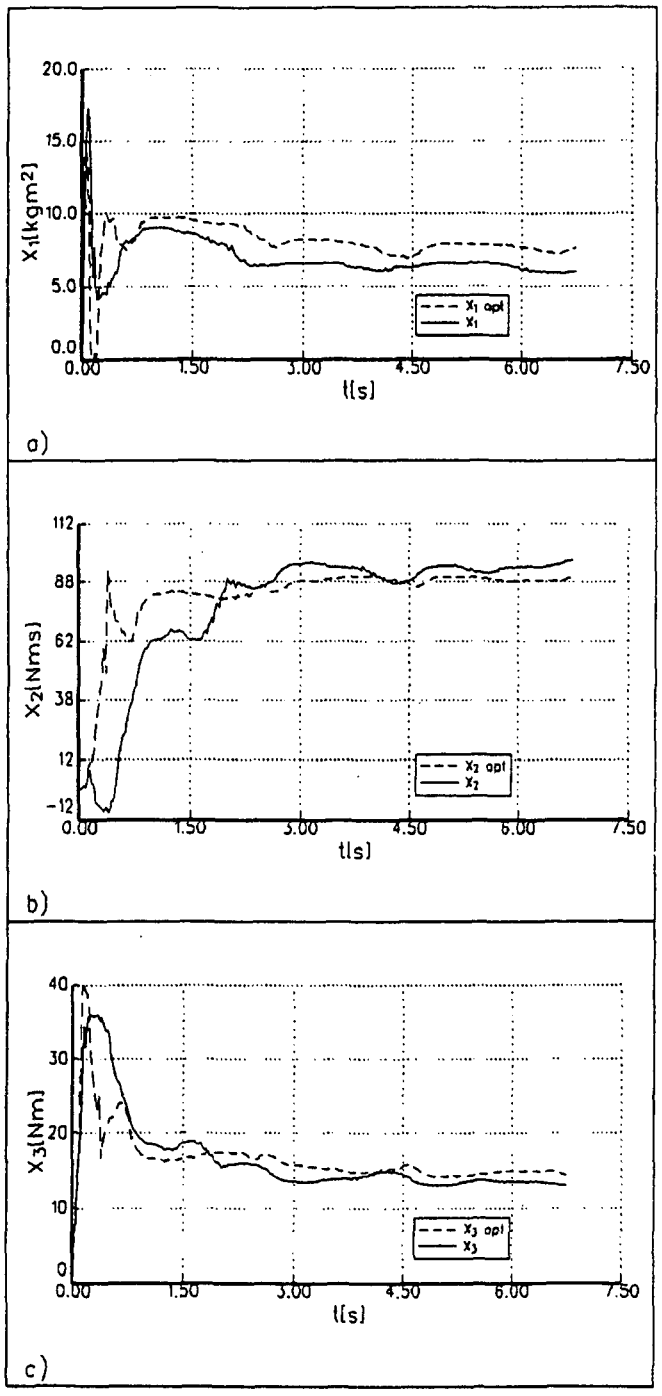

Fig. 15. a) Mass parameter identification with optimal and non-optimal trajectories for the first joint, b) Coulomb parameter identification with optimal and non-optimal trajectories for the first joint, c) Velocity friction parameter identification with optimal and non-optimal trajectories for the first joint.

measured and simulated trajectories, except Kallenbach,[49] and Pfeiffer and Hölzl.[52] This comparison is more valid since the simulated trajectories are calculated by integrating the estimated inverse model. Inaccuracies of the estimated parameters usually cause the simulated trajectory to be much different from the measured trajectory; this has not been observed in our case.

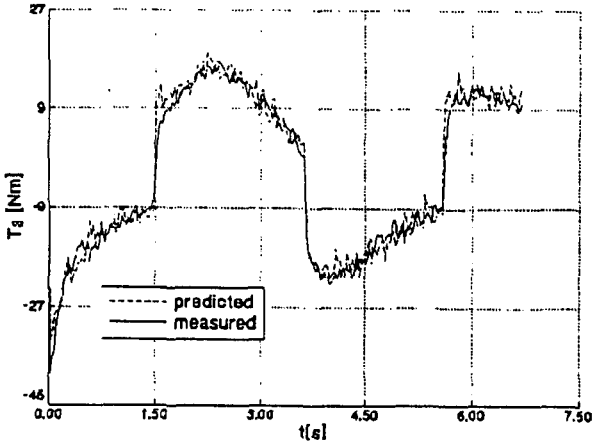

Fig. 16. Measured and predicted torques for the third joint.

7. CONCLUDING REMARKS

In this study we have presented the exciting trajectories for dynamic robot and load parameters identification experiments. As a criterion we have used the minimization of the condition number of the information matrix. We have applied this criterion to different identification problems in robotics. We have used it in two models: differential and integral. We have compared the results with those existing in the robotics literature. For the integral model we have tried short and long integrals. Exciting trajectories are very important for the integral model due to loss of information in this model in comparison with the differential model. Therefore we have run several numerical experiments particularly for this model for both robot and load dynamic parameters identification. We argue that a trial and error method in choosing an exciting trajectory does not necessary always give good results. This phenomenon was observed in the process of load identification. Some initial trajectory were chosen close to optimal; for example, we have chosen some trajectories with initial condition number as low as 181 which could not be improved by the optimization procedure. The numerical results were

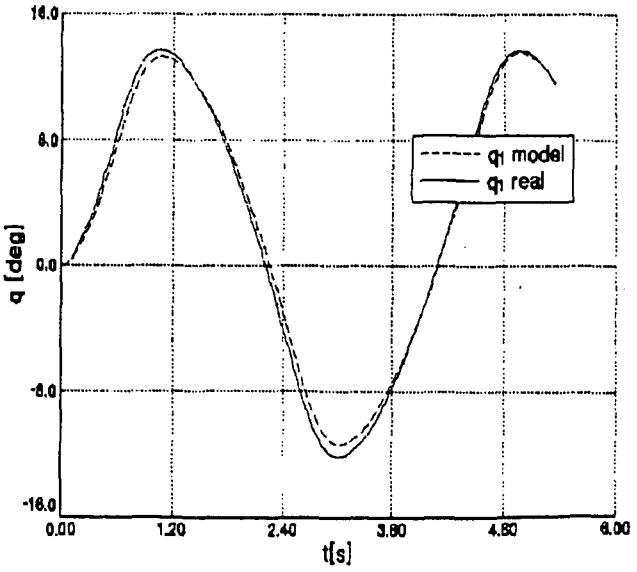

Fig. 17. Measured and simulated positions for the first joint.

successfully verified by the experimental results with the IRp-6 industrial robot.

References

1. C.H. An, C.G. Atkeson and J.M. Hollerbach, *Model-Based Control of a Robot Manipulator* (The MIT Press, Cambridge, 1988).
2. M. Gautier and W. Khalil, "On the Identification of the Inertial Parameters of Robots" *Proc. of the 27th CDC,* Austin, USA, (1988) pp. 2264–2269.
3. P.K. Khosla, "Real-Time Control and Identification of Direct-Drive Manipulators" *Ph.D. Thesis* (Carnegie-Mellon University, 1986).
4. K. Kozłowski and M. Prüfer, "Parameter Identification of an Experimental 2-Link Direct Drive Arm" *Proc. of the IASTED International Conference, Control and Robotics,* Vancouver, Canada (1992) pp. 313–316.
5. H.B. Olsen and G.A. Bekey, "Identification of Robot Dynamics" *Proc. of the 1986 IEEE International Conference on Robotics and Automation,* San Francisco, USA (1986) pp. 1004–1010.
6. K. Kozłowski, "Identification of Model Parameters of Robotic Manipulators" *Systems Science* **18,** No. 1–2, 165–187 (1992).
7. B. Armstrong-Hélouvry, *Control of Machines with Friction,* (Kluwer Academic Publishers, Holland, 1991).
8. K. Kozłowski and P. Dutkiewicz, "Identification of Friction and Robot Dynamics for a Class of Geared Robots" *Proc. of the Fourth International Symposium on Measurement and Control in Robotics,* Smolenice, Slovakia (1995) pp. 301–306.
9. P. Dutkiewicz, K. Kozłowski and W. Wróblewski, "Experimental Identification of Robot and Load Dynamics Parameters" *Proc. of the 2-nd IEEE Conference on Control Applications,* Vancouver, Canada (1993a) pp. 767–776.
10. Z. Lu, K.B. Shimoga and A.A. Goldenberg, "Experimental Determination of Dynamic Parameters of Robotic Arms", *J. Robotic Systems* **10,** No. 8, 1009–1029.
11. M. Prüfer and F. Wahl, "Analyse und Vorkompensation von Reibungseffecten bei Industrieroboten mit Getrieben" *VDI Berichte,* No. 1094, 597–605 (1993).
12. G. Seeger and W. Leonhard, "Estimation of Rigid Body Models for a Six-Axis Manipulator with Geared Electric drives" *Proc. of the IEEE International Conference on Robotics and Automation,* Scottsdale, USA (1989) pp. 1690–1695.
13. S. Seeger, "Self-Tuning Control of a Commercial Manipulator Based on An Inverse Dynamic Model" *Proc. of the Symposium on Robot Control SYROCO'91,* Vienna, Austria (1991) pp. 453–458.
14. I. Ha, M. Ko and S.K. Kwon, "An Efficient Estimation Algorithm for the Model Parameters of Robotic Manipulators" *IEEE Transactions on Robotics and Automation* **5,** 386–394 (1989).
15. R. Specht and P. Isermann, "On-Line Identification of Inertia, Friction and Gravitational Forces Applied to an Industrial Robot" *IFAC Proceedings Series 1989, SYROCO'88,* Karlsruhe, Germany (1988) pp. 219–224.
16. M. Prüfer and F. Wahl, "Friction Analysis and Modelling for Geared Robots", *Preprints of the Fourth Symposium on Robot Control,* Capri, Italy (1994) pp. 551–556.
17. W. Khalil and J.F. Kleinfinger, "Minimum Operations and Minimum Parameters of the Dynamic Models of Tree Structure Robots" *IEEE J. Robotics and Automation* **RA-3,** No. 6, 517–526 (1987).
18. Shih-Ying Sheu and M.W. Walker "Identifying the Independent Inertial Parameter Space of Robot Manipulators" *J. Robotics Research* **10,** No. 6, 618–683 (1991).
19. M. Gautier and W. Khalil "A Direct Determination of Minimum Inertial Parameters of Robots" *Proc. of the IEEE International Conference on Robotics and Automation,* Philadelphia, USA (1988) pp. 1682–1686.
20. M. Gautier and W. Khalil, "Identification of the Minimum Inertial Parameters of Robots" *Proc. of the IEEE International Conference on Robotics and Automation,* Scottsdale, USA (1989) pp. 1529–1534.
21. H. Mayeda, K. Yoshida and K. Osuka, "Base Parameters of Manipulator Dynamic Models" *IEEE Transactions on Robotics and Automation* **6,** No. 3, 313–321 (1990).
22. H. Mayeda, K. Osuka and A. Kangawa, "A New Identification Method for Serial Manipulator Arms" *Preprints IFAC 9th World Congress 4,* Budapest, Hungary (1984) pp. 74–79.
23. M. Gautier and C. Presse, "Sequential Identification of Base Parameters of Robots", *Proc. of the Fifth International Conference on Advanced Robotics,* Pisa, Italy, (1991) 1105–1110.
24. M. Gautier, W. Khalil and P.P. Restrepo, "Identification of the Dynamic Parameters of a Closed Loop Robot" *Proc. of the 1995 IEEE International Conference on Robotics and Automation,* Nagoya, Japan (1995) pp. 3045–3050.
25. F. Caccavale and P. Chiacchio, "Energy-Based Identification of Dynamic Parameters for a Conventional Industrial Manipulator" *Preprints of the Fourth IFAC Symposium on Robot Control,* Capri, Italy (1994) pp. 619–624.
26. M. Prüfer, C. Schmidt and F. Wahl, "Identification of Robot Dynamics with Differential and Integral Models: A Comparison" *Proc. of the IEEE International Conference on Robotics and Automation,* San Diego, USA (1994) pp. 340–345.
27. C. Presse and M. Gautier, "Identification of Robot Parameters via Sequential Energy Method" *Proc. of the Third IFAC Symposium on Robot Control,* Vienna, Austria (1991) pp. 117–122.
28. C. Canudas de Wit, K.J. Aström and K. Braun, "Adaptive Friction Compensation in DC-Motor Drives" *IEEE Journal of Robotics and Automation* **RA-3,** 681–685 (1987).
29. C. Canudas de Wit, P. Noël, A. Aubin and B. Brogliato, "Adaptive Friction Compensation in Robot Manipulators: Low Velocities", *J. Robotics Research* **10,** 189–199 (1991).
30. J. Schaefers, S.J. Xu and M. Darouach, "On Parameter Estimation of Industrial Robots Without Using Acceleration Signal" *Proc. of 10th IFAC Symposium on System Identification,* Copenhagen, Denmark, (1994) pp. 589–593.
31. W. Szynkiewicz, A. Gosiewski and D. Janecki, "Experimental Verification of Dynamics Model of the IRp-6 Robot Manipulator" *Proc. of the Second National Conference on Robotics and Automation* (in Polish), Wrocław, Poland (1990) pp. 255–260.
32. G.W. Van Der Linden and A.J.J. Van der Weiden, "Practical Rigid Body Parameter Estimation" *Preprints of the Fourth IFAC Symposium on Robot Control,* Capri, Italy (1994) pp. 631–636.
33. M. Gautier, W. Khalil, C. Presse and P.P. Rastrepo, "Experimental Identification of Dynamic Parameters of Robot" *Preprints of the Fourth IFAC Symposium on Robot Control,* Capri, Italy (1994) pp. 625–630.
34. U. Zimmermann, H. Wunderlich, H. Rake and M. Bruns, "Identification of Time Varying Parameters of the Robot Dynamics" *IFAC Proc. Series 1989, SYROCO'88,* Karlsruhe, Germany (1989) pp. 225–229.
35. S.K. Lin, "Identification of a Class of Nonlinear Deterministic Systems with Application to Manipulators" *IEEE Transactions on Automatic Control* **39,** No. 9, 1886–1893 (1994).
36. S.K. Lin, "An Identification Method for Estimating the Inertia Parameters of a Manipulator" *J. Robotics Systems* **9,** No. 4, 505–528 (1992).
37. F. Caccavale and P. Chiacchio, "Identification of dynamic Parameters for a Conventional Industrial Manipulator"

Proc. of the 10th IFAC Symposium on System Identification, Copenhagen, Denmark (1994) pp. 583–588.
38. P. Dutkiewicz, K. Kozłowski and W. Wróblewski, "Experimental Identification of Load Parameters" *Proc. of the IEEE International Symposium on Industrial Electronics*, Budapest, Hungary (1993b) pp. 361–366.
39. I.M.Y. Mareels et al., "How Exciting Can a Signal Really Be" *Systems and Control Letters* **8**, 197–204 (1987).
40. G.H. Golub and C.F. Van Loan, *Matrix Computation* (John Hopkins University Press, Baltimore, MD, 1989).
41. B. Armstrong, "On Finding Exciting Trajectories for Identification Experiments Involving Systems with Nonlinear Dynamics" *J. Robotics Research* **8**, 28–48 (1989).
42. P.O. Vandanjon, M. Gautier and P. Desbats, "Identification of Robots Inertial by Means of Spectrum Analysis" *Proc. of the 1995 International Conference on Robotics and Automation*, Nagoya, Japan (1995) pp. 3033–3038.
43. C. Presse and M. Gautier, "New Criteria of Exciting Trajectories for Robot Identification" *Proc. of the IEEE International Conference on Robotics and Automation*, Atlanta, USA (1993) pp. 907–912.
44. M. Gautier and W. Khalil, "Exciting Trajectories for the Identification of Base Inertial Parameters of Robots" *J. Robotics Research* **11**, 362–375 (1992).
45. M. Gautier, "Optimal Motion Planning for Robot's Inertial Parameters Identification" *Proc. of the 31st IEEE Conference on Decision and Control*, Tucson, USA (1992) pp. 70–73.
46. K. Kozłowski and P. Dutkiewicz, "Optimal Trajectory Design for the Identification of Robot and Load Dynamics" *Appl. Math. and Comp. Sci.* **5**, No. 4, 671–687 (1995).
47. P. Dutkiewicz, K. Kozłowski and W. Wrólewski, "Robot Programming System for Research Purposes" *Proc. of the COMPUEURO'93*. Paris-Evry, France (1993c) pp. 94–101.
48. M. Gautier, "Identification of Robot Dynamics" *Proc. of the IFAC/IFIP/IMACS International Symposium on Theory of Robots*, Vienna, Austria (1986) pp. 351–356.
49. R. Kallenbach, *Kovarianzmethoden zur Parameteridentification Zeitkontinuierlicher Systeme* (VDI Verlag, 1987).
50. S. Wolfram, *Mathematica, a System for Doing Mathematics* (Addison Wesley Publishing Company, 1992).
51. C. Canudas de Wit and A. Aubin, "Robot Parameter Identification via sequential Hybrid Algorithm" *Proc. of the IEEE International Conference on Robotics and Automation*, Sacramento, USA (1991) pp. 952–957.
52. F. Pfeiffer and J. Hölzl, "Parameter Identification for Industrial Robots" *Proc. of the 1995 IEEE International Conference on Robotics and Automation*, Nagoya, Japan (1995) pp. 1468–1475.